Appl. Phys. B 88, 1–4 (2007)
DOI: 10.1007/s00340-007-2678-7

**Applied Physics B**
**Lasers and Optics**

C. VON KORFF SCHMISING[1,✉]
M. BARGHEER[1]
M. KIEL[1]
N. ZHAVORONKOV[1]
M. WOERNER[1]
T. ELSAESSER[1]
I. VREJOIU[2]
D. HESSE[2]
M. ALEXE[2]

# Accurate time delay determination for femtosecond X-ray diffraction experiments

[1] Max-Born-Institut für Nichtlineare Optik und Kurzzeitspektroskopie, 12489 Berlin, Germany
[2] Max-Planck-Institut für Mikrostrukturphysik, Weinberg 2, 06120 Halle, Germany

**Received: 19 February 2007/Revised version: 19 April 2007**
**Published online: 2 June 2007 •** 

**ABSTRACT** We report on a versatile and accurate method for determining the time delay between femtosecond X-ray and optical pulses in an optical pump/X-ray diffraction probe experiment. Upon excitation with moderate pump fluences, Bragg peaks of thin $SrTiO_3$ (STO)/$SrRuO_3$ (SRO) superlattices display 50% changes in diffracted X-ray intensity, followed by a pronounced lineshift ($\Delta\theta/\theta = 0.03°$) on a 10 ps time-scale. A parallel time-resolved measurement of the instantaneous all-optical reflectivity change allows for a precise temporal analysis of the fully reversible X-ray response and gives the time delay zero with an accuracy of $\pm 100$ fs.

**PACS** 61.10.Nz; 82.53.-k; 07.85.-m

## 1 Introduction

Fundamental processes in physics, chemistry and biology are governed by atomic motions and occur on a time-scale set by vibrational periods, typically a few hundred femtoseconds. In order to study (optically induced) non-equilibrium structures, considerable effort has been made to develop novel X-ray sources like third generation synchrotrons, free electron lasers and laser-driven plasma sources [1]. Short X-ray pulses of high brilliance and pulse lengths down to the subpicosecond range allow for a growing number of time-resolved X-ray absorption and diffraction experiments. In general, such experiments are based on a pump–probe scheme, where an optical pump pulse excites atomic motion and a time-delayed X-ray probe pulse takes a snapshot of the moving structure [2–7].

Pump–probe studies with femtosecond time resolution require ultrashort optical and X-ray pulses with a relative timing jitter that is negligible compared to the pulse durations. In addition, temporal pulse spreading and time delays originating from the group velocity mismatch in the sample have to be minimized, e.g., by reducing the sample thickness. Such requirements call for methods that quantitatively analyze the time envelopes and the delay of the pulses at the location of the sample.

So far, there is no practical method to accurately and quickly determine such quantities. Experiments with accelerator based X-ray sources require a synchronized femtosecond laser that provides the pump pulses. The jitter between the X-ray pulses and an external pump laser pulse has been measured indirectly by an electro-optical sampling technique that records the arrival time of electron bunches with subpicosecond accuracy [8] but does not provide the timing of the X-ray pulse at the location of the sample. For experiments with laser driven plasma sources, where optical pump and X-ray probe pulses are intrinsically synchronized, one may use a sample showing a fast X-ray response upon excitation to infer time-delay zero. Along those lines, changes of X-ray diffraction signals due to non-thermal melting [9–11] and/or strain generation in semiconductors [12] have been analyzed to derive the time delay between pump and probe pulses. This method is hampered by the irreversible character of the pump-induced structural changes, requiring a fresh sample volume for each pump pulse and, thus, limiting the maximum possible pulse repetition rate. Furthermore, the assumption of an instantaneous sample response may be invalid.

In this letter, we present an accurate, sensitive and easily implementable method to determine the absolute time delay between optical pump and X-ray probe pulses. The pump pulse induces fully reversible lattice dynamics in a nanolayered metallic/dielectric superlattice (SL) which is monitored by diffracting X-ray probe pulses of variable delay from the sample. For moderate pump fluences of $\leq 10\,\mathrm{mJ/cm^2}$, the SL peaks of the diffraction pattern display strong intensity changes of up to 50% with kinetics that remain unchanged for a wide range of pump intensities. A comparative measurement of the pump-induced optical reflectivity change is made using a probe pulse traveling along the path of the X-ray-probe pulse. It shows an instantaneous electronic response which enables a timing calibration of the optical pump and X-ray-probe pulses with a $\pm 100$ fs accuracy. With such a calibration, the SL can be used to determine delay zero in

✉ Fax: +49-30-6392-1489, E-mail: korff@mbi-berlin.de

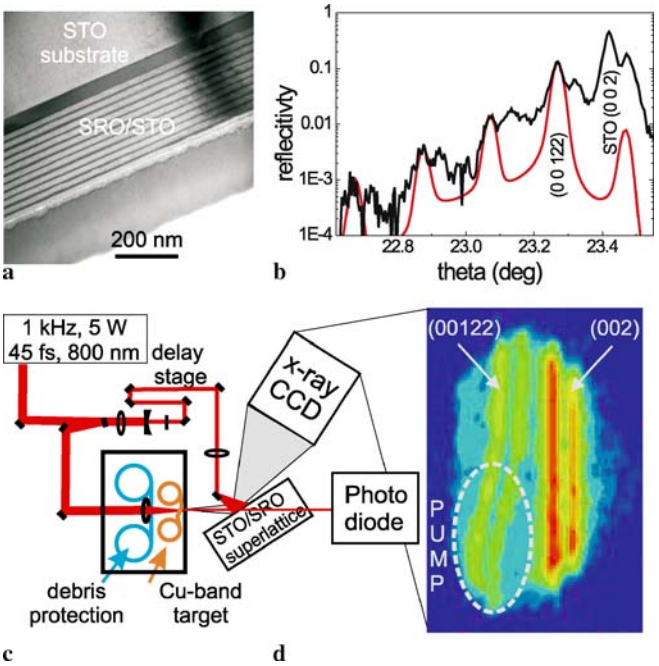


**FIGURE 1** (**a**) TEM cross section of the STO/SRO superlattice. (**b**) Measured static X-ray reflectivity curve of the STO/SRO superlattice on a STO substrate (*black, solid*) and simulation based on dynamic X-ray diffraction theory calculated for Cu $K_{\alpha 1}$ (*red, solid*). (**c**) Schematic of the pump–probe setup. (**d**) CCD image of the (002) reflex of the STO substrate and the (00 122) superlattice peak. Clearly visible is the optically induced, reversible lineshift of the lower part of the sample

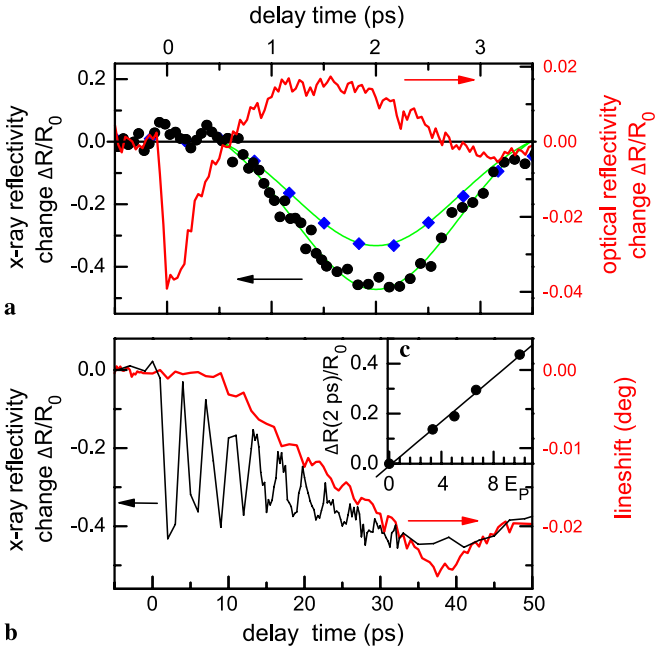


**FIGURE 2** (**a**) Transient intensity modulation for an excitation density of 10 mJ/cm$^2$ (*circles, black*) and 7 mJ/cm$^2$ (*diamond, blue*). The *red line* shows the dielectric response of the superlattice sample. (**b**) The reflectivity change of the (00 122) reflection shows damped oscillation up to 30 ps around a decreased absolute reflectivity. Lineshift (*red line*) in degrees of the (00 122) reflection as a function of pump–probe time delay. (**c**) Linear dependence of the reflectivity change after 2 ps as function of the pump fluence $E_P$ in mJ/cm$^2$

other experiments, particularly when simultaneous all-optical measurements are impossible.

## 2 Experiment

A $SrTiO_3$ (STO)/$SrRuO_3$ (SRO) SL consisting of 10 pairs of STO/SRO layers of $d_{STO} = 17.9$ nm/$d_{SRO} = 6.3$ nm thickness each (Fig. 1a) is used for measuring the time delay between optical pump and X-ray probe pulses. The nanometer periodicity $d_{SL} = d_{STO} + d_{SRO}$ of the SL results in additional Bragg peaks at multiples of $g = 2\pi/d_{SL}$ [13], some of which are shown in Fig. 1b. In the time-resolved experiments, a femtosecond optical pulse induces fully reversible changes of the SL geometry, i.e. layer thicknesses. Such changes are probed by diffracting a subpicosecond X-ray pulse from the sample and recording changes of intensity and angular position of a SL peak. As the X-ray signal originates exclusively from the SL with a very small total thickness of $d = 10\, d_{SL} = 242$ nm, distortions of the pump–probe timing and/or temporal pulse envelopes by group velocity dispersion are negligible. Moreover, the small sample thickness allows for a homogeneous excitation of the SL by the pump pulse.

Our pump–probe setup (Fig. 1c) is based on a Ti:sapphire laser system delivering 45 fs pulses with an energy of 5 mJ at a repetition rate of 1 kHz and a wavelength of 800 nm. 94% of the laser power is focused on a 20 µm thick moving Cu tape target to generate hard X-ray bursts containing $10^8$ photons at the characteristic Cu $K_{\alpha 1}$ and $K_{\alpha 2}$ energy in a pulse of approximately 100 fs duration [14, 15]. The divergent X-ray emission emerging from a target area of 10 µm diameter in the forward direction is diffracted by the sample aligned for the (00 122) superlattice peak at a Bragg angle $\theta = 23.27°$ and recorded by a CCD-camera covering the respective $2\theta$ region. For measurement of the X-ray transient, a beam splitter picks the remaining 6% of the laser pulse which is then sent over a delay stage to control the pump–probe delay. It is collimated onto the sample to produce a fluence of up to 10 mJ/cm$^2$ and covers the lower part of the sample as indicated in Fig. 1d[1]. The diffracted X-ray signal is accumulated for 3 s for each value of the time delay. Within this integration time roughly $10^5$ photons are diffracted, corresponding to a peak reflectivity of 10% with an angular width of 0.04°.

For the comparative measurement of the transient optical reflectivity of the SL sample, the Cu target and the 10 µm thick Al seal of the vacuum chamber are removed. The probe pulse that normally generates the X-rays is attenuated by closing an iris. The probe pulse path is otherwise left unchanged. The attenuated 800 nm probe beam hits the SL sample at the same position as the X-ray pulses and the reflected intensity is measured as a function of pump–probe delay $t$.

Time-resolved data is summarized in Fig. 2. The red line in Fig. 2a represents the optical reflectivity change $\Delta R(t)/R_0 = (R(t) - R_0)/R_0$ as a function of the pump–probe delay. $R(t)$ and $R_0$ are the reflectivities of the SL sample with and without excitation by the 800 nm pump pulse, respectively. A narrow pulse-limited decrease of reflectivity occurs around delay zero. The pump-induced electronic polarization

[1] The reduction of time resolution due to the non-collinear pump–probe geometry is negligible.

decays with a dephasing time short compared to the pulse duration, resulting in an 'instantaneous' nonlinear response of the sample. The initial reflectivity change is followed by slower contributions due to carrier redistribution and phonon oscillations.

The circular symbols in Fig. 2a and the black line in Fig. 2b represent the transient changes of the angle-integrated X-ray reflectivity $\Delta R/R_0$ on the (00 122) SL Bragg peak for an excitation density of 10 mJ/cm$^2$. The X-ray reflectivity reaches a minimum after approximately 30 ps and at earlier time delays is superimposed by damped oscillations of large amplitude and a 3.2 ps period. The first oscillation maximum with a value of $\Delta R/R_0 = -0.5$ occurs at 2 ps after the delay zero derived from the nonlinear optical response. The absolute value of $\Delta R/R_0$ depends linearly on the pump fluence (inset Fig. 2c). The time evolution of $\Delta R/R_0$, however, remains unchanged for pump fluences of 3 to 10 mJ/cm$^2$ (cf. diamond symbol curve in Fig. 2a, which had a pump fluence of 7 mJ/cm$^2$). The high accuracy of the all-optical pump–probe trace and the optical pump/X-ray probe measurements allows for linking the two pump–probe delay scales with an accuracy of $\pm 100$ fs. It should be noted that our technique avoids any ad-hoc assumptions concerning the time evolution of the X-ray reflectivity change. Delay zero is determined very precisely even for the non-instantaneous rise of the signal in Fig. 2a.

In addition to the change of X-ray reflectivity, there is a gradual shift of the angular position of the SL Bragg peaks (Fig. 2b). The line shift sets in after 5 to 10 ps, reaches a maximum of $\theta = 0.025°$ after approximately 30 ps and extends over several hundreds of picoseconds. This effect may be useful for generating rough initial estimates of delay zero when setting up experiments.

## 3 Discussion

These results demonstrate that our technique yields the pump–probe timing in ultrafast X-ray diffraction experiments with very high accuracy. In the following, we briefly discuss the physics underlying the structural response of the SL sample. The static X-ray diffraction pattern (Fig. 1b) consists of the (002) Bragg peak of the STO-substrate and a series of SL peaks at multiples of $g = 2\pi/d_{\mathrm{SL}}$ which are split according to the doublet of the Cu $K_{\alpha 1}$ and $K_{\alpha 2}$ radiation. Their peak intensities are dictated by the structure factor, which sensitively depends on the relative thickness of the SRO and STO layers within one layer pair (SL unit cell). The 800 nm pump pulse couples predominantly to the electrons in the metallic SRO layer, leading to an electronic excitation with a spatial periodicity $g$ and, via electron–phonon coupling, generating coherent SL motions with wavevector $\boldsymbol{g}$ [5]. The electronic excitation in the SRO layer leads to a non-instantaneous build-up of stress and identical experiments with superlattices of different layer-thicknesses (not shown) demonstrate that the measured rise-time of approximately 0.5 ps is an intrinsic property of SRO which originates from the microscopic processes generating lattice elongations after electronic excitation. The complex electron–phonon coupling scenario is still under investigation and a detailed analysis will be published elsewhere. The resulting periodic compression and expansion of the SRO and STO layers changes the structure factor and leads to the observed X-ray intensity modulation of the SL peaks. The oscillation period is determined by the time it takes a sound wave to travel through one SRO/STO layer pair, $T = d_{\mathrm{SRO}}/v_{\mathrm{SRO}} + d_{\mathrm{STO}}/v_{\mathrm{STO}}$, where $v_{\mathrm{SRO}}$ and $v_{\mathrm{STO}}$ are the sound velocities. The maximal change in reflectivity of $\Delta R/R_0 = -0.5$ corresponds to a strain amplitude of $\Delta a/a_0 = 3 \times 10^{-3}$. The angular positions of the SL peaks start to shift after 5–10 ps (Fig. 2b) when the total SL thickness changes on a time scale determined by strain propagation through the entire structure.

## 4 Conclusion

In conclusion, we have presented a versatile and accurate method to determine the pulse timing in optical pump/X-ray diffraction probe experiments. After photoexcitation, a 0.25 μm thick superlattice shows a strong reversible modulation of the diffracted X-ray intensity. Its rise in time is calibrated by comparison with the all-optical reflectivity change. The transient X-ray diffraction patterns and the frequency of superlattice phonons can be tailored over a wide range by epitaxial growth techniques [16, 17], allowing for further optimization as well as customization beneficial for a broad range of applications in ultrafast X-ray science.

## REFERENCES


1 R. F. Service, Science **298**, 1356 (2002)
2 A. Rousse, C. Rischel, J. C. Gauthier, Rev. Mod. Phys. **73**, 17 (2001)
3 M. Bargheer, N. Zhavoronkov, M. Woerner, T. Elsaesser, Chem. Phys. Chem. **7**, 783 (2006)
4 K. Sokolowski-Tinten, C. Blome, J. Blums, A. Cavalleri, C. Dietrich, A. Tarasevitch, I. Uschmann, E. Förster, M. Kammler, M. Horn-von-Hoegen, D. von der Linde, Nature **422**, 287 (2003)
5 M. Bargheer, N. Zhavoronkov, Y. Gritsai, J.C. Woo, D.S. Kim, M. Woerner, T. Elsaesser, Science **306**, 1771 (2004)
6 C. Bressler, M. Chergui, Chem. Rev. **104**, 1781 (2004)
7 L.X. Chen, Ann. Rev. Phys. Chem. **56**, 221 (2005)
8 A.L. Cavalieri, D.M. Fritz, S.H. Lee, P.H. Bucksbaum, D.A. Reis, J. Rudati, D.M. Mills, P.H. Fuoss, G.B. Stephenson, C.C. Kao, D.P. Siddons, D.P. Lowney, A.G. MacPhee, D. Weinstein, R.W. Falcone, R. Pahl, J. Als-Nielsen, C. Blome, S. Düsterer, R. Ischebeck, H. Schlarb, H. Schulte-Schrepping, Th. Tschentscher, J. Schneider, O. Hignette, F. Sette, K. Sokolowski-Tinten, H.N. Chapman, R.W. Lee, T.N. Hansen, O. Synnergren, J. Larsson, S. Techert, J. Sheppard, J.S. Wark, M. Bergh, C. Caleman, G. Huldt, D. van der Spoel, N. Timneanu, J. Hajdu, R.A. Akre, E. Bong, P. Emma, P. Krejcik, J. Arthur, S. Brennan, K.J. Gaffney, A.M. Lindenberg, K. Luening, J.B. Hastings, Phys. Rev. Lett. **94**, 114 801 (2005)
9 C.W. Siders, A. Cavalleri, K. Sokolowski-Tinten, C. Toth, T. Guo, M. Kammler, M. Horn von Hoegen, K.R. Wilson, D. von der Linde, C.P.J. Barty, Science **286**, 1340 (1999)
10 K. Sokolowski-Tinten, C. Blome, C. Dietrich, A. Tarasevitch, M. Horn von Hoegen, D. von der Linde, A. Cavalleri, J. Squier, M. Kammler, Phys. Rev. Lett. **87**, 225 701 (2001)
11 A.M. Lindenberg, J. Larsson, K. Sokolowski-Tinten, K.J. Gaffney, C. Blome, O. Synnergren, J. Sheppard, C. Caleman, A.G. MacPhee, D. Weinstein, D.P. Lowney, T.K. Allison, T. Matthews, A.L. Cavalieri, D.M. Fritz, S.H. Lee, P.H. Bucksbaum, D.A. Reis, J. Rudati, P.H. Fuoss, C.C. Kao, D.P. Siddons, R. Pahl, J. Als-Nielsen, S. Düsterer, R. Ischebeck, H. Schlarb, H. Schulte-Schrepping, Th. Tschentscher, J. Schneider, D. von der Linde, O. Hignette, F. Sette, H.N. Chapman, R.W. Lee, T.N. Hansen, S. Techert, J.S. Wark, M. Bergh, G. Huldt, D. van der Spoel, N. Timneanu, J. Hajdu, R.A. Akre, E. Bong, P. Krejcik, J. Arthur, S. Brennan, K. Luening, J.B. Hastings, Science **308**, 392 (2005)

12 C. Rose-Petruck, R. Jiminez, T. Guo, A. Cavalleri, C.W. Siders, F. Raksi, J.A. Squier, B.C. Walker, K.R. Wilson, C.P.J. Barty, Nature **398**, 310 (1999)
13 C. Colvard, R. Merlin, M.V. Klein, A.C. Gossard, Phys. Rev. Lett. **45**, 298 (1980)
14 N. Zhavoronkov, Y. Gritsai, M. Bargheer, M. Woerner, T. Elsaesser, F. Zamponi, I. Uschmann, E. Förster, Opt. Lett. **30**, 1737 (2005)
15 N. Zhavoronkov, Y. Gritsai, G. Korn, T. Elsaesser, Appl. Phys. B **79**, 663 (2004)
16 M. Dawber, C. Lichtensteiger, M. Cantoni, M. Veithen, P. Ghosez, K. Johnston, K.M. Rabe, and J.-M. Triscone, Phys. Rev. Lett. **95**, 177 601 (2005)
17 I. Vrejoiu, G. Le Rhun, L. Pintilie, D. Hesse, M. Alexe, U. Gösele, Adv. Mater. **18**, 1657 (2006)